Performance Analysis of Indoor Vehicular VLC Links for Autonomous Driving

Elizabeth Eso*, Elnaz Alizadeh Jarchlo†, Zabih Ghassemlooy*, Stanislav Zvanovec‡,
Falko Dressler†, Juna Sathian*
*Optical Communication Research Group, Department of Mathematics, Physics and Electrical Engineering,
Northumbria University, Newcastle, UK
†Telecommunication Networks Group, School of Electrical Engineering and Computer Science,
TU Berlin, Berlin, Germany
‡Department of Electromagnetic Field, Czech Technical University, Prague, Czech Republic
{elizabeth.eso, z.ghassemlooy, juna.sathian}@northumbria.ac.uk,
{alizadeh, dressler}@ccs-labs.org, xzvanove@fel.cvut.cz

***Abstract*—One of the major challenges in indoor vehicular visible light communications (VVLC) links is associated with the mobility leading to frequent handovers, consequently resulting in increased latency and processing time. Therefore, to address this challenge, an acceptable light coverage within the indoor channel, i.e., cell planning, is of paramount importance. In this paper we investigate the performance of a VLC link for an autonomous indoor vehicle and provide insights on the impact of the distance between light access points, and the light client's (LC's) angular field of view (AFOV) employing an imaging optical concentrator with a photodiode. We derive a mathematical expression to determine the optimum AFOV of the LC as a function of other system parameters such as the vertical link distance and incidence angles. Results show step responses in the bit-error-rate (BER) performance as the incidence angle increases outside the AFOV of the LC with the BER degrading sharply from 3.8×10^{-3} to 4.4×10^{-1} with a small increment in the incidence angle over 7.35 °.**

***Index Terms*—Vehicular visible light communications, angular field of view, light access point, acceptable light coverage**

I. Introduction

Recently, there have been a number of research studies on visible light communications (VLC) as a complementary solution to other existing wireless communication technologies for indoor environments [1]–[4]. One of the main advantages of using VLC is providing a more secure network in contrast with radio frequency (RF) since the ray beams do not penetrate the walls [3], [5], [6]. Moreover, it does not interfere with the RF cellular networks. VLC is a green technology using light-emitting-diodes (LEDs), liquid crystal displays, etc as the optical Tx and photodiodes (PDs) or cameras as the optical receivers (Rx).

Autonomous indoor vehicles (AIV) and automated guided vehicles are used in several places to ease delivery of materials, e.g., in industrial automation. Considering an indoor network environment, there is less impact of the ambient light on the performance of a vehicular VLC (VVLC) network in comparison to outdoor scenarios, where the link performance can be degraded by sunlight [7], fog [8], or turbulence [9]. However, in an indoor network environment, there is a high probability for the VVLC link to experience blockage due to obstacles. Importantly, the performance of the system is highly dependent on system parameters, such as the link span, transmit power, and the field of view (FOV) of the Tx and the Rx. Moreover, aside the link quality, which is usually determined by the signal-to-noise ratio (SNR), connectivity is the key, which relies on the illumination coverage area of the Tx and/or the angular field of view (AFOV) of the light client (LC) (i.e. Rx), and the transmit power of the light source. These can all be efficiently designed to satisfy both illumination and robust data communication requirements in indoor environments. Consequently, this study aims to investigate the contribution of critical parameters such as the inter light access point (LAP) or Tx spacing, the required AFOV, the vertical link span, which depends on the height of the room/hall and the Rx, on the coverage area and the performance of the communication link employing an imaging Rx.

The remainder of this paper is organized as follows: Section II discusses related research works, while Section III presents the system model and setup for this work. In Section IV, the simulation results are presented, and finally, conclusions are given in Section V.

II. Related Work

The impact of key illumination factors such as the transmit power and the dimming factor on the coverage probability of a VLC network were investigated in [10]. The work focused on investigating the parameters that affected the system's full connectivity coverage at a horizontal plane inside an empty room, i.e., with no blocking of the line of sight (LOS) path. The authors assumed a scenario with N transmitting nodes uniformly distributed on the ceiling for illumination and data transmission. Each Tx consisted of a LED array with a symmetrical light radiation pattern. Parameters such as the room area in the range from 30 to 60 m^2, transmit power from 80 to 200 mW, light source luminaries with half power angle from 25 to 45°, error probability from 10^{-9} to 10^{-3} were

examined to provide full illumination coverage inside indoor environments.

In [11], a comprehensive lighting configuration for efficient indoor VLC networks was discussed and proposed to support mobility and link switching with a constraint on illumination, received power, and SNR. The work (i) highlighted the significance of the recognition of the impacts of the AFOV of the Rx on the connectivity performance in practical indoor scenarios; and (ii) investigated the impact of the light overlap area between two light sources with respect to the link switching (handover) process. The results obtained showed that, the proposed configuration can achieve higher communication link quality and full mobility, thus enhancing the link switching process in indoor VLC with sufficient illumination levels. In [12], the received optical power distribution of a generalized indoor VLC system was analysed by considering ceiling-mounted and wall-mounted light layouts. Numerical results showed that, using LEDs with narrow luminous intensity patterns led to larger received power variations and shorter optimal receiving distances for the ceiling-mounted LED layout. This was in contrast to smaller received power variations and longer optimal receiving distances for the wall-mounted LED layout. In [13], an angle diversity transmitter (ADT) was implemented for an indoor VLC system, named VLC-ADT. Results of the error performance analysis of the proposed VLC-ADT system were presented for the LOS link in a downlink environment considering various Rx locations in the room. The proposed system reduces the disparity between the minimum and maximum received SNR which was observed at an optimum half power angle.

To achieve an improved network throughput and communication coverage in indoor VVLC systems, we consider the impact of various system parameters on the performance. We then derive mathematical expressions to calculate the (i) optimum AFOV of the LC as a function of other system parameters, which is key to achieve improved coverage and connectivity; and (ii) received power with an imaging optical concentrator (OC) at the Rx side. In the case of a non-imaging Rx based link, the received power varies with the position of the Rx with respect to the Tx, which is highly dependent on the radiation pattern of the Tx. However, in the case of an imaging Rx based link (i.e., an image sensor-based Rx or an imaging OC used in front of the PD) the received power profile is totally different. The reason for this is that an image of the Tx is projected to the PD. Therefore, the received power remains constant, as far as the Tx is within the AFOV and directly faces the LC with no tilting angle which was not considered in the aforementioned works, hence this is investigated in this paper. Other merits of an imaging-based Rx includes spatial filtering of unwanted light sources, which is achievable by controlling the AFOV of the LC, hence dis-enabling interference from other LAPs not in the AFOV of the LC.

III. System Model and Analytical Evaluation

VLC system modeling is essential as it provides insight into the performance of the VLC links under varying system parameters as in any other wireless communications. We consider a cell with multiple LAPs and an AIV, which is the LC with a Rx that employs an imaging OC to increase the optical power density and focus the light onto the PD. Figure 1 depicts the configuration of an indoor VVLC system. To obtain the required semi-AFOV for the LC to capture n number of LAPs at any time, we need to consider the inter LAP distance l_1, the width of the LAP l_{LAP}, and the horizontal and vertical link spans denoted as l_0 and h_0, respectively. Consequently, we derive a mathematical expression for the semi-AFOV required for the Rx to capture the full image of n LAPs when an imaging OC is used at the Rx, which is given as:

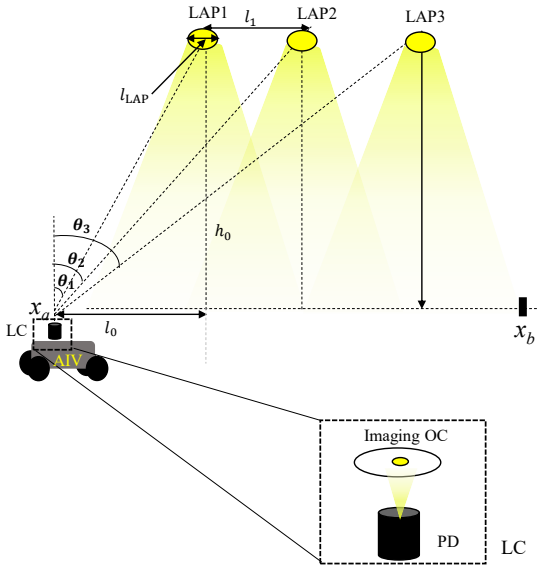

Figure 1. Configuration of an indoor VVLC system.

$$\theta_n = \arctan\left(\frac{l_1(n-1) + l_0 + l_{\mathrm{LAP}}/2}{h_0}\right) \tag{1}$$

Note that, for atleast half of the Tx image to be captured, $l_{\mathrm{LAP}}/2$ in equation (1) should be omitted.

The received signal for the LOS, can be expressed as [15]:

$$y(t) = Rx(t) * h(t) + n(t), \tag{2}$$

where $h(t)$ is the channel impulse response, R is PD's responsivity, $x(t)$ is the transmitted signal, and $n(t)$ is the additive white Gaussian noise. The area of the projected focused image of the light source A_{img} by the converging imaging OC depends on the actual area of the light source A_{LAP}, the focal length of the lens f, and the link span, which can be expressed as:

$$A_{\mathrm{img}} = A_{\mathrm{LAP}} \frac{f^2}{{h_0}^2} \tag{3}$$

Table I
KEY SIMULATION PARAMETERS

Parameter	Value
Optical transmit power P_t	0.5 W
Transmission coefficient of lens T_{lens}	0.92
Noise spectral density N_0	10^{-21} W/Hz [15]
Vertical link span h_0	5-9 m
Length of LAP l_{LAP}	5 cm
Inter-LAP distance l_1	10- 100 cm
Bit rate	100 Mbps
Focal length of OC	15, 35 mm
PD responsivity R	0.54 A/W
PD area A_{PD}	$1.96 \times 10^{-6}\text{m}^2$
Diameter of PD D_{PD}	2×10^{-3} m

Next, the received power at the PD for the LOS path can be expressed as:

$$P_r = T_{\text{lens}} \frac{A_{\text{img}}}{A_{\text{LAP}}} P_t \tag{4}$$

where T_{lens} is the transmission coefficient of the lens. For the intensity modulation and direct detection scheme with the on-off keying format and a PD-based optical Rx, the SNR and the BER are given, respectively, as [14]:

$$\text{SNR} = \frac{(P_r R)^2}{R_b N_0} \tag{5}$$

$$\text{BER} = Q\sqrt{(\text{SNR})} \tag{6}$$

where R_b is the bit rate, N_0 is the noise spectral density, and $Q(x)$ is the Q-function used for the calculation of the tail probability of the standard Gaussian distribution. Note, the theoretical BER equation (i.e. equation (6)) assumes a zero intensity for OFF symbols. Notably, the SNR is dependent on the size of the LAP's image captured, which also depends on f, AFOV and the link span and apparently also the light intensity which depends on the transmit power. The semi-AFOV of the LC in terms of f and the PD's dimensions D_{PD} (for a rectilinear imaging OC) can be expressed as [7]:

$$\phi_{\text{S-AFOV}} = \arctan\left(\frac{D_{\text{PD}}}{2f}\right) \tag{7}$$

$$\phi_{\text{S-AFOV}} = \begin{cases} \phi_{\text{ver}}, & D_{\text{PD}} = h_{\text{PD}}, \\ \phi_{\text{hor}}, & D_{\text{PD}} = w_{\text{PD}}, \\ \phi_{\text{diag}}, & D_{\text{PD}} = \sqrt{h_{\text{PD}}^2 + w_{\text{PD}}^2}, \end{cases} \tag{8}$$

where w_{PD} and h_{PD} denotes the width and height of the PD (i.e., the PD dimensions) and ϕ_{ver}, ϕ_{hor} and ϕ_{diag} is the vertical, horizontal and diagonal semi-AFOVs of the LC, respectively.

IV. SIMULATION RESULTS

We simulate based on parameters given in Table I and present the results of the required semi-AFOV as a function of the vertical link span for h_0= 5 m and for a number of LAPs and shown in Figure 2. From this Figure it can be observed that the semi-FOV decreases exponentially with the vertical link span and increases with the inter LAP spacing. For example, for n = 2 and h_0 = 5 m, the required semi-AFOV increases

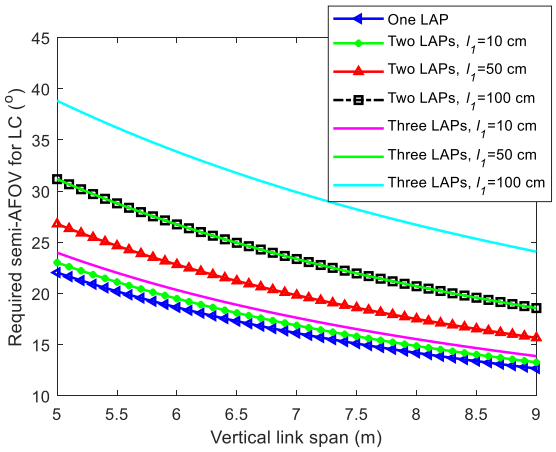

Figure 2. Required LC's AFOV as a function of vertical link span for different numbers of LAPs and inter LAP distances.

from 23.0 to 26.8 and to 31.2° as l_1 increase from 10 to 50 cm and to 100 cm, respectively. Also, it is apparent that the required AFOV drops with decrease in the number of LAPs to be captured at a time. For instance, at h_0 of 7 m, the required semi-AFOV of the LC to capture at least one, two, and three LAPs are 16.1, 23.8, and 29.9°, respectively for l_1= 100 cm.

Next, we simulate the received optical power and the BER as the AIV moves along a horizontal path from the point x_a to x_b with three LAPs on the ceiling, as depicted in Figure 1. Using equations (3) and (4) and the parameters shown in Table I, the received power as a function of the incidence angle for two inter LAP distances and vertical link spans (i.e., considering two different building heights) is depicted in Figure 3. As can be seen in Figure 3, the received power varies based on the amount of light captured by the imaging OC, which depends on its AFOV. As the AIV moves from the point x_a to x_b, the following capturing scenarios are possible (i) a single LAP; (ii) two LAPs; (iii) three LAPs; (iv) part of one or more LAPs but not the full one; (v) part of one or more LAPs in addition to a full LAP or LAPs; and (vi) no LAPs are captured by the LC.

Notably, the link with the lens with higher f (i.e., 35 mm) provides a higher received power at some points along x_a to x_b. This comes at the cost of a lower coverage angle (i.e. AFOV) and some dark spots, where no light is incident on the PD, compared with the link using a lens with lower f (i.e., 15 mm).

For example, in Figure 3(a) the maximum incidence angle after which no LAPs are further captured at the Rx (i.e., all the LAPs are beyond the AFOV of the LC) at l_1 = 20 cm are 5.9 and 7.4° for f of 35 and 15 mm, respectively. Also, the link with a longer inter LAP spacing has a wider coverage angle with no dead zones i.e., no link discontinuity with f of 15 mm compared with the link with f of 35 mm experiencing some dead zones in between the LAPs. In order to capture the full image of longer length LAPs (e.g. tubes), the AFOV requirement will increase. However, depending on the P_t, the PD's sensitivity and link span, capturing part of the Tx may be

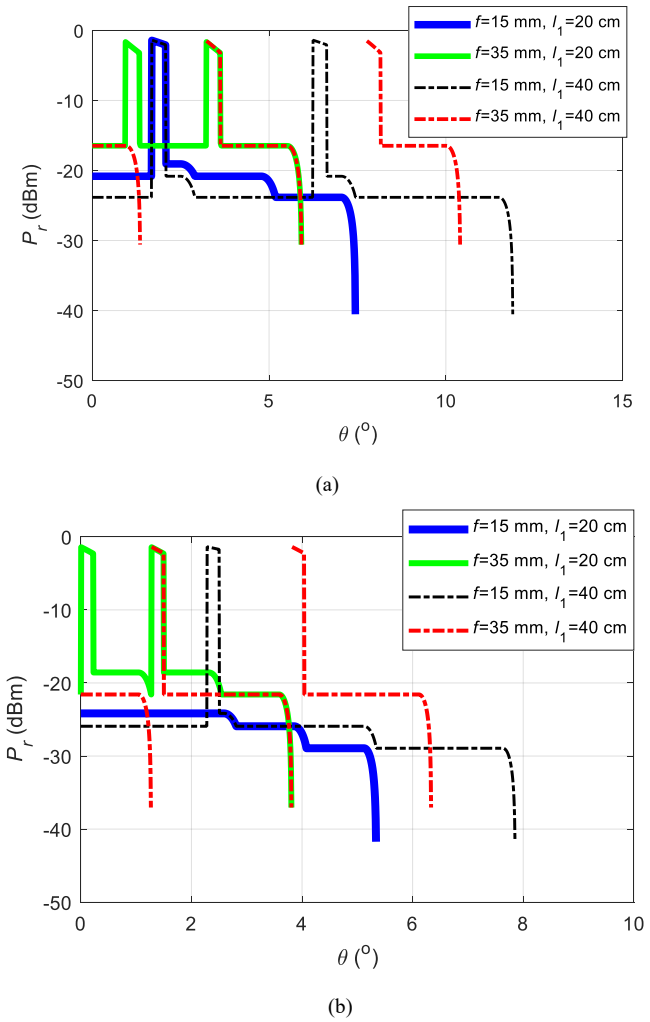

Figure 3. Received power as a function of the angle of incidence for: (a) h_0= 5 m, and (b) h_0= 9 m

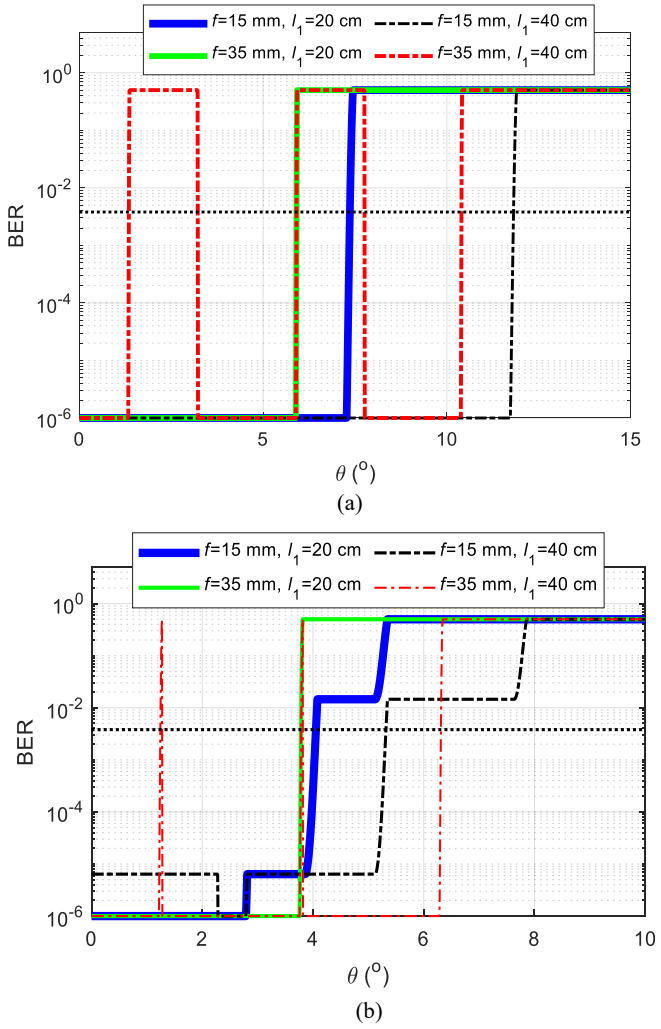

Figure 4. BER as a function of the angle of incidence for: (a) h_0= 5 m, and (b) h_0= 9 m

sufficient enough to obtain a target throughput, hence, a link power budget analysis is essential to ascertain appropriate trade-offs between system parameters to satisfy system requirements.

The BER plots are depicted in Figure 4. As can be observed, the BER degrades sharply as soon as the light source is beyond the AFOV of the Rx and improves greatly when the next LAP is captured as the image of the captured LAP is projected onto the PD. For example, as the AIV moves from x_a to x_b, (see Figure 1), for the link with f = 35 mm and l_1 = 20 cm, the BER at θ of 7.35° is 3.8 × 10^{-3} and degrades sharply to 4.4 × 10^{-1} with a small change in θ (i.e., 7.44°), see Figure 4(a).

Also, some dead zones are experienced as shown in Figure 4 i.e., the communication link is completely lost as the BER increases to 0.5. Note that, this is more evident in the link with higher f as the LC's AFOV is lower. For example, for the link with f = 35 mm and l_1 = 40 cm, the BER is above the forward error correction BER limit of 3.8 × 10^{-3} at θ of 1.4-3.2° and 5.9-7.8° and beyond 10.4°. Notably, a higher f of the lens provides a higher received power as the size of a LAP's image projected to the PD is larger when a LAP is within its AFOV than for lower f but at the expense of a lower achievable link AFOV, consequently appropriate values for each system parameter need to be determined to satisfy the system requirements. It is also noteworthy that, the required AFOV drops with the increasing vertical link span. Hence for tall buildings, the AFOV requirements drop, where sufficient optical power levels at the Rx is more desirable because of longer transmission length, compared with smaller building. Consequently, to maintain the data rate at a target BER and to reduce the need for frequent handovers in autonomous indoor VVLC systems, an acceptable communication coverage area and at the target SNR must be achieved, which significantly varies based on the system parameters and hence the need for cell planning, which would involve geometrical and link power budget analysis for proper system design.

V. Conclusion

We investigated the impact of various system parameters such as the inter LAP distance, the focal length of the imaging OC employed at the LC (i.e., the LC's AFOV), the vertical link distance and incidence angles on the performance of an autonomous indoor VVLC network. Moreover, to determine the LC's AFOV required to capture n number of LAPs at a time, we derived a mathematical expression to calculate the optimum AFOV based on the inter-LAP spacing, the vertical and horizontal link spans, and the size of the LAP. Results obtained showed step responses in the BER performances as the AIV moved along the communication path. For instance, for the link with h_0 = 5 m, f = 35 mm and l_1 = 20 cm, the BER degraded sharply from 3.8×10^{-3} to 4.4×10^{-1} for very little increment in θ from 7.35 to 7.44 °.

VI. Acknowledgment

This work was supported by the European Union's Horizon 2020 research and innovation programe under the Marie Sklodowska-Curie grant agreement no 764461 (VisIoN). It is also based upon work from COST Action CA19111 NEWFOCUS, supported by COST (European Cooperation in Science and Technology).

References

[1] J. Lian, Z. Vatansever, M. Noshad, and M. Brandt-Pearce, "Indoor visible light communications, networking, and applications," *Journal of Physics: Photonics*, vol. 1, no. 1, p. 012 001, Jan. 2019.

[2] F. Wang, Z. Wang, C. Qian, L. Dai, and Z. Yang, "Efficient Vertical Handover Scheme for Heterogeneous VLC-RF Systems," *IEEE/OSA Journal of Optical Communications and Networking*, vol. 7, no. 12, p. 1172, Dec. 2015.

[3] G. A. Mapunda, R. Ramogomana, L. Marata, B. Basutli, A. S. Khan, and J. M. Chuma, "Indoor Visible Light Communication: A Tutorial and Survey," *Wireless Communications and Mobile Computing*, vol. 2020, pp. 1–46, Dec. 2020.

[4] E. Alizadeh Jarchlo, E. Eso, H. Doroud, A. Zubow, F. Dressler, Z. Ghassemlooy, B. Siessegger, and G. Caire, "FDLA: A Novel Frequency Diversity and Link Aggregation Solution for Handover in an Indoor Vehicular VLC Network," *IEEE Transactions on Network and Service Management (TNSM)*, 2021, online first: 10.1109/TNSM.2021.3075476.

[5] S. Shao, A. Khreishah, M. B. Rahaim, H. Elgala, M. Ayyash, T. D. Little, and J. Wu, "An Indoor Hybrid WiFi-VLC Internet Access System," in *11th IEEE International Conference on Mobile Ad Hoc and Sensor Systems (MASS 2014)*, Philadelphia, PA: IEEE, Oct. 2014.

[6] L. U. Khan, "Visible light communication: Applications, architecture, standardization and research challenges," *Digital Communications and Networks*, vol. 3, no. 2, pp. 78–88, May 2017.

[7] E. Eso, Z. Ghassemlooy, S. Zvanovec, J. Sathian, and A. Gholami, "Fundamental Analysis of Vehicular Light Communications and the Mitigation of Sunlight Noise," *IEEE Transactions on Vehicular Technology (TVT)*, 2021.

[8] M. Elamassie, M. Karbalayghareh, F. Miramirkhani, R. C. Kizilirmak, and M. Uysal, "Effect of Fog and Rain of the Performance of Vehicular Visible Light Communications," in *87th IEEE Vehicular Technology Conference (VTC 2018-Spring)*, Porto, Portugal: IEEE, Jun. 2018.

[9] E. Eso, Z. Ghassemlooy, S. Zvanovec, J. Sathian, M. M. Abadi, and O. I. Younus, "Performance of Vehicular Visible Light Communications under the Effects of Atmospheric Turbulence with Aperture Averaging," *Sensors*, vol. 21, no. 8, p. 2751, Apr. 2021.

[10] A. Vavoulas, H. G. Sandalidis, T. A. Tsiftsis, and N. Vaiopoulos, "Coverage Aspects of Indoor VLC Networks," *Journal of Lightwave Technology*, vol. 33, no. 23, pp. 4915–4921, Dec. 2015.

[11] T.-C. Bui, S. Kiravittaya, K. Sripimanwat, and N.-H. Nguyen, "A Comprehensive Lighting Configuration for Efficient Indoor Visible Light Communication Networks," *International Journal of Optics*, vol. 2016, pp. 1–9, 2016.

[12] Y. Wang, M. Chen, J.-Y. Wang, J. Shi, Z. Yang, Y. Pan, and R. Guan, "Impact of LED transmitters' radiation pattern on received power distribution in a generalized indoor VLC system," *Optics Express*, vol. 25, no. 19, p. 22 805, Sep. 2017.

[13] V. Dixit and A. Kumar, "Performance Analysis of Indoor Visible Light Communication System with Angle Diversity Transmitter," in *4th IEEE Conference on Information & Communication Technology (CICT 2020)*, Chennai, India: IEEE, Dec. 2020.

[14] J. Kahn and J. R. Barry, "Wireless Infrared Communications," *Proceedings of the IEEE*, vol. 85, no. 2, pp. 265–298, Feb. 1997.

[15] M. K. Hasan, M. Z. Chowdhury, M. Shahjalal, V. T. Nguyen, and Y. M. Jang, "Performance Analysis and Improvement of Optical Camera Communication," *Applied Sciences*, vol. 8, no. 12, p. 2527, Dec. 2018.